ACS APPLIED MATERIALS & INTERFACES

Research Article

www.acsami.org

Supercritical Hydrothermal Synthesis and In situ Organic Modification of Indium Tin Oxide Nanoparticles Using Continuous-Flow Reaction System

Jinfeng Lu,[†] Kimitaka Minami,[†] Seiichi Takami,[‡] Masatoshi Shibata,[§] Yasunobu Kaneko,[§] and Tadafumi Adschiri*[,†,‡]

[†]Advanced Institute for Materials Research, WPI, and [‡]Institute of Multidisciplinary Research for Advanced Materials, Tohoku University

[§]Idemitsu Kosan Co., Ltd.

Supporting Information

ABSTRACT: ITO nanoparticles were synthesized hydrothermally and surface modified in supercritical water using a continuous flow reaction system. The organic modification of the nanoparticles converted the surface from hydrophilic to hydrophobic, making the modified nanoparticles easily dispersible in organic solvent. The addition of a surface modifier into the reaction system impacted the crystal growth and particle size as well as dispersion. The particle size was 18 nm. Highly crystalline cubic ITO with a narrow particle size distribution was obtained. The advantages of short reaction time and the use of a continuous reaction system make this method suitable for industrial scale synthesis.

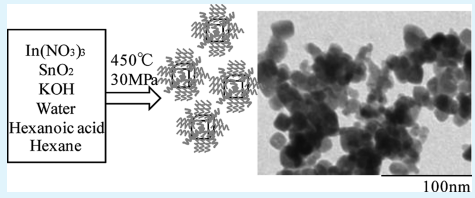

KEYWORDS: *ITO, supercritical condition, surface modification, nanoparticles, flow reaction system, environmentally benign technology*

INTRODUCTION

Tin-doped indium oxide (ITO) has been widely applied in photoelectronic products such as liquid-crystal displays (LCD), polymer electronics as organic photodiodes (OPD), thin film transistors (TFT), solar cells.[1−4] Its popularity arises from its properties of high electrical conductivity combined with high optical transparency in the visible spectral range, making it suitable for use as a transparent electrode which is fundamental in many optoelectronic devices.

ITO transparent electrodes traditionally have been deposited on flexible or heat-sensitive substrates using gas-phase deposition techniques.[5] However, with the rising price of indium metal and significant loss of ITO during conventional thin film deposition procedures, printing techniques such as inkjet printing that utilize ITO nanoparticles are expected to supplant the conventional method. Accordingly, interest in the production and use of ITO nanoparticles has steadily increased over the past few years. Using printing technology, ITO film can be fabricated more effectively and cheaply with less ITO loss.[6,7] When dispersing ITO nanoparticles into the ink, the inkjet printer can create an electric circuit directly onto the substrate. The critical issue in this type of printing technology is preparing nanosize particles, which can be homogeneously dispersed in a solvent.[8]

Typical transparent, electron conductive nanoink consists of ITO nanoparticles dispersed in solvent and mixed with a binder. Reducing the particle size to the order of nanometers improves the ITO film surface by diminishing haze and roughness and enhancing the transparency because of the suppression of Rayleigh scattering. The main difficulty lies in fabricating nanoparticles that will homogeneously disperse in solvent, as they tend to aggregate because of high surface energy. This property is adaptable through surface modification, which must be compatible with the rest of the fabrication process, including a low temperature curing. This has been problematic for particle films, as it has been reported that the sheet resistance of an ITO particle film after hardening under UV-irradiation at low temperature (<130 °C) was decreased to 1 kΩ /sq.[9] ITO nanoparticles are expected to help solve these problems, and may also improve upon the qualities of the conventional ITO coated films, which have only about 80% transmission in the visible light range.[10]

There have been several preparation methods of ITO nanoparticles reported, including low temperature coprecipitation, solvothermal synthesis, hydrothermal synthesis, and others.[11−16] However, there have been no methods developed that can maintain continuous production in an environmentally benign manner, and this is of crucial importance to establishing production at an industrial scale.

Supercritical continuous-flow reaction systems (SCFRS) offer a green route to producing metal oxide particles. A series of metal oxide nanoparticles has been synthesized in supercritical water.[17−19] Fang et al. synthesized nanocrystalline indium and tin oxide in supercritical water,[20] although the indium conversion rate was low (28.7%), they did not achieve a single phase ITO, nor did they attempt to utilize surface

Received: October 16, 2011
Accepted: December 1, 2011
Published: December 1, 2011

modification. In our group, we have established a novel process for the simultaneous synthesis and in situ modification of metal oxide nanoparticles under supercritical conditions.[21−23] We found that limiting crystal growth creates small, well-dispersed particles that resist aggregation, which can be accomplished by fabrication in supercritical water and modification with organic-ligand molecules. For this purpose, we employed this method of supercritical hydrothermal synthesis with SCFRS for the synthesis of well-dispersed ITO nanoparticles with a hydrophobic surface.

In this report, we describe the preparation and surface modification of highly crystalline ITO nanoparticles using organic molecules in supercritical water as the reaction medium. Additionally, we discuss dispersion and optoelectronic properties of these surface-modified ITO nanoparticles.

EXPERIMENTAL SECTION

$In(NO_3)_3$ was purchased from Shinko Chemical Co., Ltd. SnO_2 sol (8 wt %, pH =9.5−10.5, average of particle size: 2 nm) was from Taki Chemical Co., Ltd. KOH was from High Purity Chemicals Co., Ltd. Formic acid, hexanoic acid, and hexane were from Wako Chemicals, Ltd. The precursor solutions were prepared by dissolving $In(NO_3)_3$ and SnO_2 sol (molar ratio In:Sn = 9:1) in distilled water. To this mixture was slowly added KOH solution to obtain a white colored sol, the pH was adjusted to 7, and the precursor sol was diluted with distilled water to 0.1 M. 1.0 M formic acid in aqueous solution was prepared. Hexanoic acid used as modifier was dissolved in hexane to a concentration of 0.2 M.

The experiments were performed using a flow type stainless 316 steel reactor, as depicted in Figure.1. The system pressure was

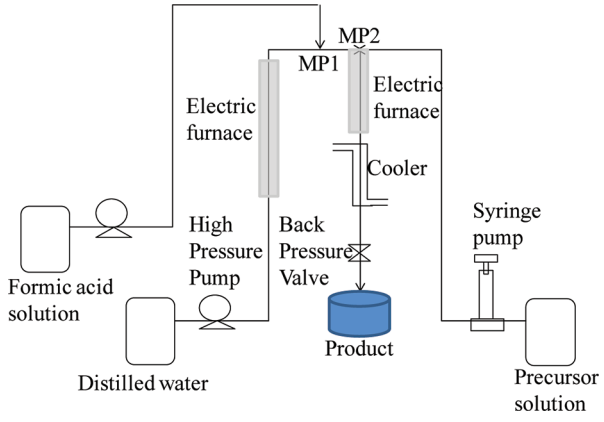

Figure 1. Schematic diagram of the flow reaction system.

maintained at 30 MPa using a backpressure regulator. Preheated high temperature water was fed into the reactor (36 mL/min) and mixed with 1.0 M formic acid fed from another line (4 mL/min) at mixing point 1 (MP1). Next, 0.1 M precursor sol or the mixture with modifier solution fed by the other line (4 mL/min) was added to this mixed solution at mixing point 2 (MP2). Subsequently, the solution was heated rapidly to the reaction temperature. The solution mixture was passed through a tube reactor and then quenched to room temperature by a cooling water jacket. The product solution was depressurized with a backpressure regulator and collected at the outlet. The reaction time (τ) was calculated based on the volume (V), flow rate (F), and density (ρ) of the solution in the tube reactor ($\tau = V/(F\rho)$). In this experiment, the reaction times for different temperature conditions were 22 s for 350 °C, 12 s for 400 °C, and 7 s for 450 °C.

The phases of the nanoparticles were characterized by X-ray diffractometry (XRD-Rigaku) using Cu Kα radiation. The particle size and morphology of the particles were examined using transmission electron microscopy (TEM(EDX)-Hitachi). The energy-dispersive X-ray (EDX) spectrum of samples was obtained using energy dispersive X-ray microanalysis (EDAX-AMETEK) combined with TEM. The electric resistance of the ITO samples was measured using a powder resistance measurement system (MCP-MCCAT). The conductivity was calculated from the measured resistance.

RESULTS AND DISCUSSION

As illustrated in Figure 1, the precursor sol was mixed with preheated water at MP2 to heat it rapidly to the reaction temperature (350, 400, and 450 °C). Figure 2A shows XRD

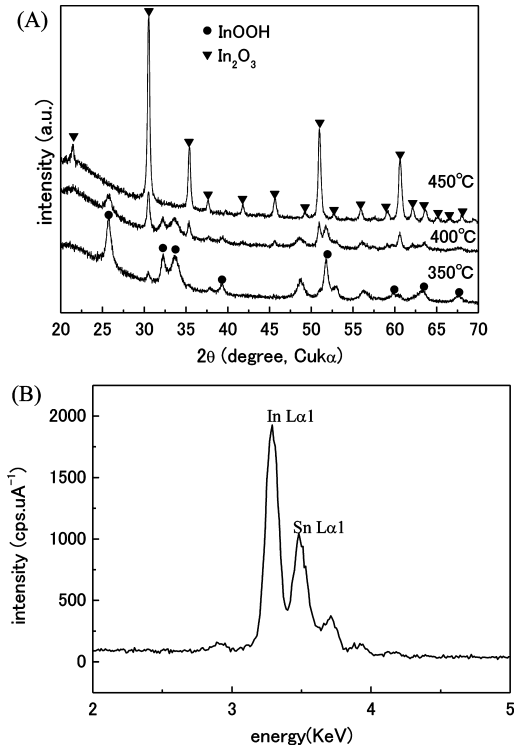

Figure 2. (A) XRD pattern of indium tin oxide (ITO) prepared at 350, 400, and 450 °C. (B) EDX spectrum of sample obtained at 450 °C.

patterns of samples obtained at these three temperatures. Temperatures below 400 °C produced mixed phases of cubic In_2O_3 and InOOH, but with increasing temperature, the peak of cubic In_2O_3 increased and that of InOOH became smaller, indicating a better yield of cubic In_2O_3. When the temperature was increased to 450 °C, a single phase was obtained. Compared with pure In_2O_3 (JCPDS Card No. 71−2195), the peaks were shifted to slightly lower values (Table S1 in the Supporting Information), indicating an increase in the size of the unit cell, indicating that Sn^{4+} might be doped into the cubic structure of In_2O_3.

In addition, EDX analysis of the nanoparticles was conducted combined with TEM image (Figure 4a). A typical EDX spectrum is shown in Figure 2B. Both In Lα1 (3.2 keV) and Sn Lα1 (3.4 keV) peaks were observed, indicating the presence of indium and tin elements in the products. The Sn/In ratio was determined to be 1:9, which matches the ratio in the precursor solution and provides further evidence of the formation of ITO. We also took the EDX analysis in other positions, which all showed the presence of tin.

XRD results suggest that InOOH nuclei form in the beginning of the reaction and upon dehydration generate

dx.doi.org/10.1021/am2014234 | ACS Appl. Mater. Interfaces 2012, 4, 351−354

cubic In_2O_3. Temperature plays an important role in the formation of single phase ITO nanoparticles in the very short reaction time under supercritical conditions. Because of the remarkable decrease in water density as the temperature increases rapidly to 450 °C, the dehydroxylation from $In(OH)_3$ to InOOH and the final transformation to cubic In_2O_3 proceed rapidly. Conversely, at temperatures lower than 400 °C, the dehydration does not occur efficiently and thus the transformation from InOOH to In_2O_3 is incomplete.

In the next step in nanoparticle fabrication, to generate the reducing atmosphere needed for increasing the oxygen vacancy in ITO, formic acid solution was fed into MP1 where it combined with preheated supercritical water at 500 °C. Yu et al. has studied the thermal decomposition of formic acid at temperatures between 320 and 500 °C and pressures between 17.8 and 30.3 MPa,[24] and they reported that at 420 °C, the conversion of HCOOH reached 100% in a short reaction time to give the major products CO_2 and H_2. In supercritical water, the equilibrium of this reaction shifts toward the products CO_2 + H_2: H_2O + CO ⇆ HCOOH ⇆ CO_2 + H_2. These gases are miscible with supercritical water to form a homogeneous phase. Consequently, H_2 and CO_2 gases derived from the formic acid provide a good reducing atmosphere inside the tube reactor. Subsequently, the precursor sol was added into the reaction system at MP2 at a temperature of 450 °C. As shown in Figure

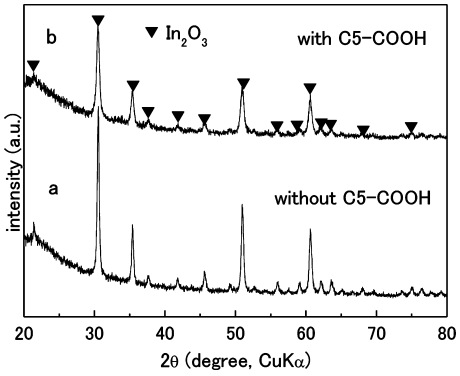

Figure 3. XRD patterns of ITO nanoparticles: (a) without modifier and (b) with modifier hexanoic acid (C5-COOH).

3, single-phase ITO was obtained under these conditions with no trace of additional phases. Furthermore, the color of the ITO nanoparticles changed from yellow to blue, which is a known indicator of a higher carrier concentration due to oxygen vacancies,[25] and is attributable to the reducing atmosphere generated by the addition of formic acid. TEM was used to assess the size of the blue ITO nanoparticles (Figure 4), which were found to be ~30 nm. However, TEM also revealed that the ITO nanoparticles were heavily aggregated, and so we proceeded to carry out in situ surface modification in the SCFRS.

Hexanoic acid solution was added to the precursor sol in a 1:2 ratio and stirred rigorously. The other conditions were kept the same, i.e., the reaction temperature was 450 °C and pressure was 30 MPa, and formic acid was again added to create a reducing atmosphere. The effect of introducing hexanoic acid into the system was that the organic ligand capped the nanoparticle surface and limited the growth of the particles. The XRD pattern of modified nanoparticles reveals that all of the peaks are lower in intensity and broadened as compared

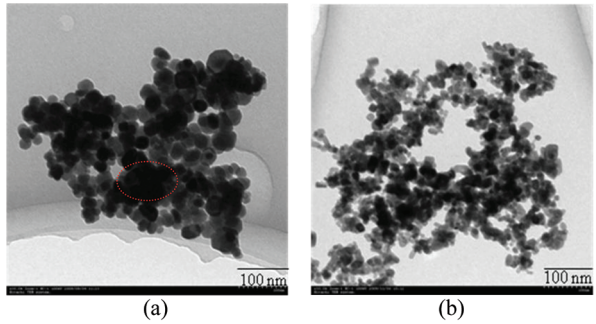

Figure 4. TEM images of samples (a) without modifier and (b) with modifier hexanoic acid. Red circle shows the region of EDX analysis.

with the pattern of nanoparticles fabricated without organic surface modification (Figure 3). The crystallite sizes of these two samples were calculated from the main peak (*hkl* = 222) of XRD data using Scherrer's equation; the unmodified nanoparticles were found to be 32 nm and the nanoparticles modified with hexanoic acid were 18 nm, demonstrating that the size of the nanoparticles was reduced by the organic ligand capping. This smaller size of the modified particles was confirmed using TEM. From the image of the modified nanoparticles (Figure 4), the size was found to be consistent with the XRD (*hkl* = 222 peak is significantly high) results, revealing cubic ITO particles with an average diameter of 18 ± 0.8 nm.

The dispersibility of ITO was investigated by putting the particles in a binary phase-separated solvent of hexane and water. As shown in Figure 5, the surface modified particles

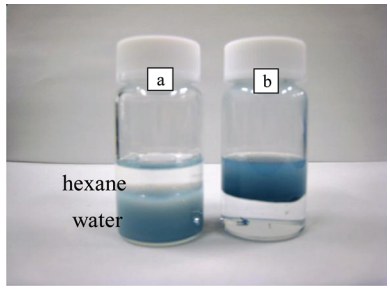

Figure 5. Dispersibility of ITO nanoparticles (a) in the absence of organic modifier and (b) in the presence of organic modifier hexanoic acid.

dispersed in organic phase, whereas the particles without surface modification dispersed in the aqueous phase of the binary solvent system. These results indicate that the organic ligand, hexanoic acid, had bound to the surface of modified ITO nanoparticles and converted them from hydrophilic to hydrophobic, although hexanoic acid may not be the best modifier.[15] We have succeeded in making a thin film by the spin-coating method for well-dispersed nanoparticles, although we have not measured the electroconductivity of the film.

For this system, it is worthwhile to understand the phase behavior and the solvent effect on the nucleation rate in the presence of organic capping agent. It is known that in the supercritical region, water becomes completely miscible with many hydrocarbons while also becoming a poor solvent for many inorganics.[26] From the pressure−temperature phase diagram for the water and hexane mixture, it is known that the mixture will become one phase above 360 °C at 30 MPa.[27]

dx.doi.org/10.1021/am2014234 | ACS Appl. Mater. Interfaces 2012, 4, 351−354

The solubility of ITO nanoparticles in this water/hexane mixture phase remains lower than in pure water, and therefore, small ITO nuclei form at an extremely high reaction rate owing to the high degree of supersaturation. The large surface energy of the nanoparticles makes them unstable, causing them to form large aggregations in the absence of an organic modifier. When the fabrication was repeated in the presence of hexanoic acid, the organic ligand capped the nanoparticle surface immediately and limited their growth and tendency for aggregation. As was reported in the previous research,[21,22] strong binding reaction occurs on the surface, which was confirmed by the TGA analysis. As a result, the particle size was controlled. The hydrophobic nature of the surface modifier allows excellent dispersion of the nanoparticles in organic solvent.

The electric resistance of ITO nanoparticles was measured isothermally at room temperature using the four-probe method. To initiate close interparticle contacts, the nanoparticles were pressed to form transparent thin pellets. The conductivity, calculated from electric resistance, is shown in Figure 6. Electric

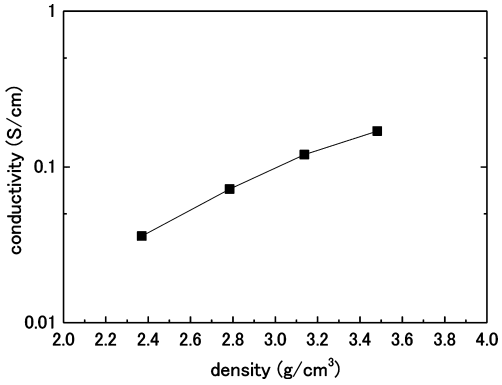

Figure 6. Change in conductivity of modified ITO.

conductivity increases gradually with increasing pressure. At a pressure of 9.6 MPa, a sheet conductivity of 1.2×10^{-1} (S/cm) was measured. This value is roughly the same as for other colloidal ITO particles reported previously, although these nanoparticles are much smaller and display better dispersibility in organic solvent.

CONCLUSIONS

We report a simple and rapid synthetic process for preparing ITO nanoparticles with simultaneous surface modification with an organic ligand by SCFRS. The surface modified particles are highly crystalline ITO nanocrystals with excellent dispersion in organic solvent. Aggregation and crystal growth were effectively suppressed by organic ligand capping. We can get 1−10 g/h under this supercritical condition.

ASSOCIATED CONTENT

Supporting Information

Table of change in peak positions for ITO compared to purdue In_2O_3. This material is available free of charge via the Internet at http://pubs.acs.org.

AUTHOR INFORMATION

Corresponding Author

*Tel & Fax: 81-22-217-6321. E-mail: ajiri@tagen.tohoku.ac.jp.

REFERENCES

(1) Hamberg, I.; Granqivst, C. G. *J. Appl. Phys.* **1986**, *60*, R123−R159.
(2) Shen, Z.; Burrows, P. E.; Bulović, V.; Forrest, S. R.; Thompson, M. E. *Science* **1997**, *276*, 2009−2011.
(3) Ng, H. T.; Fang, A.; Huang, L.; Li, S. F. Y. *Langmuir* **2002**, *18*, 6324−6329.
(4) Garcia, G.; Buonsanti, R.; Runnerstrom, E. L.; Mendelsberg, R. J.; Llordes, A.; Anders, A.; Richardson, T. J.; Milliron, D. J. *Nano Lett.* **2011**, *11*, 3315−4420.
(5) Tahar, R. B. H.; Ban, T.; Ohya, Y.; Takahashi, Y. *J. Appl. Phys.* **1998**, *83*, 2631−2645.
(6) Han, H.; Adams, D.; Mayer, J. W.; Alford, T. L. *J. Appl. Phys.* **2005**, *98*, 083705−(1−8).
(7) Liu, Q.; Lu, W.; Ma, A.; Tang, J.; Lin, J.; Fang, J. *J. Am. Chem. Soc.* **2005**, *127*, 5276−5277.
(8) Richard, A. G. Jr.; Summers, C. J. *Thin Solid Films* **2009**, *518*, 1136−1139.
(9) Puetz, J.; Aegerter, M. A. *Thin Solid Films* **2008**, *516*, 4495−4501.
(10) Heusing, S.; de Oliveira, P. W.; Kraker, E.; Haase, A.; Palfinger, C.; Veith, M. *Thin Solid Films* **2009**, *518*, 1164−1169.
(11) Kim, K. Y.; Park, S. B. *Mater. Chem. Phys.* **2004**, *86*, 210−221.
(12) Yang, J.; Li, C.; Quan, Z.; Kong, D.; Zhang, X.; Yang, P.; Lin, J. *Cryst. Growth & Des.* **2008**, *8*, 695−699.
(13) Choi, S.-I.; Nam, K. M.; Park, B. K.; Seo, W. S.; Park, J. T. *Chem. Mater.* **2008**, *20*, 2609−2611.
(14) Li, X.; Kale, G. M. *J. Phys.: Conf. Ser.* **2006**, *26*, 319−322.
(15) Giltsrap, R. A.; Capozzi, C. J.; Carson, C. G.; Gerhardt, R. A.; Summers, C. J. *Adv. Mater.* **2008**, *20*, 4163−4166.
(16) Bühler, G.; Thölmann, D.; Feldmann, C. *Adv. Mater.* **2007**, *19*, 2224−2227.
(17) Hakuta, Y.; Seino, K.; Ura, H.; Adschiri, T.; Takizawa, H.; Arai, K. *J. Mater. Chem.* **1999**, *9*, 2671−2674.
(18) Hayashi, H.; Hakuta, Y.; Kurata, Y. *J. Mater. Chem.* **2004**, *14*, 2046−2051.
(19) Lu, J.; Hakuta, Y.; Hayashi, H.; Ohashi, T.; Nagase, T.; Hoshi, Y.; Sato, K.; Nishioka, M.; Inoue, T.; Hamakawa, S. *J. Supercrit. Fluids* **2008**, *46*, 77−82.
(20) Fang, Z.; Assaaoudi, H.; Guthrie, R. I. L.; Kozinski, J. A.; Butler, I. S. *J. Am. Ceram. Soc.* **2007**, *90*, 2367−2371.
(21) Zhang, J.; Ohara, S.; Umetsu, M.; Naka, T.; Hatakeyama, Y.; Adschiri, T. *Adv. Mater.* **2007**, *19*, 203−206.
(22) Adschiri, T. *Chem. Lett.* **2007**, *36*, 1188−1193.
(23) Taguchi, M.; Takami, S.; Naka, T.; Adschiri, T. *Cryst. Growth Des.* **2009**, *9*, 5297−5303.
(24) Yu, J.; Savage, P. E. *Ind. Eng. Chem. Res.* **1998**, *37*, 2−10.
(25) Shimada, S.; Mackenzie, K. J. D. *J. Cryst. Growth* **1981**, *55*, 453−456.
(26) Watanabe, M.; Sato, T.; Inomata, H.; Smith, R. L. Jr.; Arai, K.; Kruse, A.; Dinjus, E. *Chem. Rev.* **2004**, *104*, 5803−5821.
(27) Abdulagatov, I. M.; Bazaev, A. R.; Magee, J. W.; Kiselev, S. B.; Ely, J. F. *Ind. Eng. Chem. Res.* **2005**, *44*, 1967−1984.